Satellite Products and Services Review Board

Algorithm Theoretical Basis Document: GCOM-W1/AMSR2 Precipitation Product

Compiled by the
GCOM-W1/AMSR2 Precipitation Team

Version 1.0

February, 2014

TITLE: ATBD: GCOM-W1/AMSR2 PRECIPITATION PRODUCT VERSION 1.0

AUTHORS:

Patrick Meyers (CICS-MD/ESSIC)

Suleiman Alsweiss (GST)

Letitia Soulliard (IMSG)

DOCUMENT HISTORY
DOCUMENT REVISION LOG

DOCUMENT TITLE: ATBD – GCOM-W1/AMSR2 PRECIPITATION PRODUCT			
DOCUMENT CHANGE HISTORY			
Revision No.	**Date**	**Revision Originator Project Group**	**CCR Approval # and Date**
1.0	N/A	No version 1	N/A

LIST OF CHANGES

DOCUMENT TITLE: ATBD – GCOM-W1/AMSR2 PRECIPITATION PRODUCT					
LIST OF CHANGE-AFFECTED PAGES/SECTIONS/APPENDICES					
Version Number	Date	Changed By	Page	Section	Description of Change(s)

TABLE OF CONTENTS

LIST OF TABLES AND FIGURES

LIST OF ACRONYMNS

AMSR2: Advanced Microwave Sounding Radiometer 2
CONUS: Continental United States
DDS: Data Distribution Server
EDR: Environmental Data Record
FAR: False Alarm Ratio
FOV: Field of View
GAASP: GCOM-W1 AMSR2 Algorithm Software Processor
GCOM – W1: Global Change Observation Mission 1st – Water
GPCC: Global Precipitation Climatology Centre
GPCP: Global Precipitation Climatology Project
GPDS: GCOM Processing and Distribution System
GPROF: Goddard Profiling Algorithm 2010 Version 2
IMS: Interactive Multisensor Snow and Ice Mapping System
JAXA: Japanese Aerospace Exploration Agency
NMQ: National Mosaic and Multi-Sensor QPE
OE: Optimal Estimation
OI: Optimal Interpolation
OSPO: Office of Satellite and Product Operations
PR: Precipitation Radar
POD: Probability of Detection
QPE: Quantitative Precipitation Estimate
RMSE: Root Mean-Square Error
SDR: Satellite Data Record
SST: Sea Surface Temperature
TMI: TRMM Microwave Imager
TMPA: TRMM Multi-satellite Precipitation Analysis
TPW: Total Precipitable Water
TRMM: Tropical Rainfall Measurement Mission

1. INTRODUCTION

1.1. Product Overview

1.1.1. Product Description

An accurate record of the hydrological cycle is essential for identifying duration and spatial extent of extreme events, such as droughts and flooding, as well as long-term trends of rainfall amount and distribution. The Goddard Profiling Algorithm 2010 Version 2 (GPROF) produces swath-level global rain rate estimates. GPROF calculates the surface rain rate of liquid precipitation and defines the contribution from convective precipitation. Rain rates are calculated for open ocean, coast, and snow-free land surfaces. Files are saved in 9 minute granules in netCDF format

1.1.2. Product Requirements

EDR Attribute	Threshold	Objective
Applicable conditions		Delivered under "all weather" conditions
Horizontal cell size	5 km land (89 GHz FOV); 10 km ocean (37 GHz FOV size); 5-10 km sampling	5.0 km
Mapping uncertainty, 3 sigma	< 5 km	3.0 km
Measurement range	0 – 50 mm/hr	Not Specified
Measurement precision	0.05 mm/hr	0.05 mm/hr
Measurement uncertainty	2 mm/hr over ocean; 5 mm/hr over land	2 mm/hr
Refresh	At least 90% coverage of the globe about every 20 hours (monthly average)	Not Specified
Precipitation type	Stratiform or convective	Not Specified
Latency	16 minutes	Not Specified

Table 1-1: Requirements for the NOAA GCOM-W1/AMSR2 precipitation product.

The GPROF retrieval algorithm ingests corrected L1B brightness temperatures. The ocean rainfall algorithm requires a recent optimal interpolation ¼° Sea Surface Temperature (SST) analysis (Reynolds et al. 2007). All other necessary ancillary data are static and contained within the GAASP structure.

1.2. Satellite Instrument Description

The GCOM program is part of JAXA's broader commitment toward global and long-term observation of the Earth's environment. GCOM consists of two medium-size, polar-orbiting satellite series with one-year overlap between them for inter-calibration. The two satellite series are GCOM-W (Water) and GCOM-C (Climate). Two instruments were selected as payloads for these missions to cover a wide range of geophysical parameters: AMSR2 on GCOM-W and the Second-generation Global Imager on GCOM-C. The AMSR2 instrument will perform observations related to the global water and energy cycle, while the SGLI will conduct surface and atmospheric measurements related to the carbon cycle and radiation budget (GCOM Data Users Handbook).

The GCOM-W project is a 13-year mission with three satellites in series, each with a 5-year lifetime including a 1-year overlap with follow-on satellite for calibration purposes. The GCOM-W1, launched in May 2012, will be followed by the GCOM-W2, and GCOM-W3 nominally planned for launch in 2016, and 2020, respectively.

AMSR2 onboard GCOM-W1 is a microwave radiometer system that measures dual polarized [vertical (V-pol) and horizontal (H-pol)] radiances at 6.9, 7.3, 10.65, 18.7, 23.8, 36.5, and 89.0 GHz. It is a sun-synchronous orbiter that acquires microwave radiance data by conically scanning the Earth's surface to obtain measurements along a semicircular pattern in front of the spacecraft. It operates at a nominal earth incidence angle (EIA) of 55º that results in a wide swath of 1,450 km. The aperture diameter of AMSR2 antenna is 2.0 meters with an instantaneous field of view (FOV) spatial resolution that varies inversely with frequency [13].

AMSR2 inherited most of AMSR-E characteristics with some important improvements including: a larger main reflector (compared to the 1.6m diameter of AMSR-E), the addition of the 7.3GHz channels (for C-band radio frequency interference (RFI) detection), 12 bit quantization for all channels, and improvements in the calibration system (Imaoka et al. 2010). Summarized operating characteristics of AMSR2 are shown in Table 1 and the instrument design and geometry in Figure 1.

Center Freq. (GHz)	Band Width (MHz)	Beam Width (3dB, deg.)	Ground IFOV (km)	Sampling Interval (km)
6.925/7.3	350	1.8	35×62	
10.65	100	1.2	24×42	
18.7	200	0.65	14×22	10
23.8	400	0.75	15×26	
36.5	1000	0.35	7×12	
89.0	3000	0.15	3×5	5

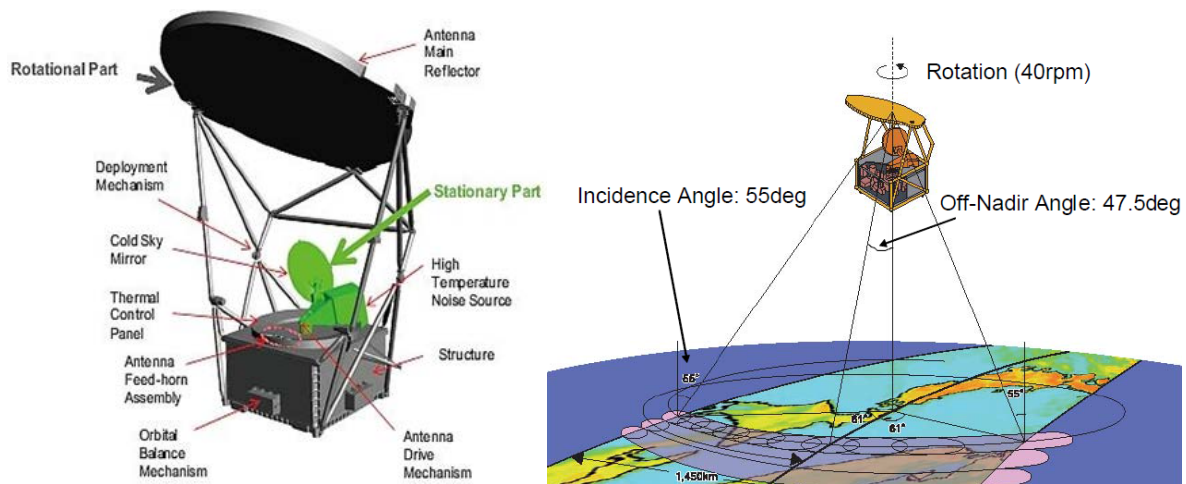Table 1-2: AMSR2 Instrument Specifications

Figure 1-1: (Left) Schematic of AMSR2 instrument. (Right) AMSR2 scan geometry (Source: JAXA).

2. ALGORITHM DESCRIPTION

GPROF was originally developed for TMI (Gopalan et al. 2010; Kummerow et al. 2011). The modular nature of GPROF allows the algorithm to be easily ported between different passive microwave imagers with comparable channels.

2.1. Processing Outline

All processing for GPROF is conducted within the GCOM-W1 AMSR2 Algorithm Software Processor (GAASP) (Figure 2-1). GAASP calibrates the AMSR2 SDR (See SDR ATBD) and ingests an external SST analysis (Reynolds et al. 2007). The GAASP GPROF preprocessor organizes the external files and sets conditions for the main GPROF retrieval algorithm. Within GPROF, each pixel is classified as land, ocean, or coast and then directed into the appropriate partition. After the pixels are screened for data quality and radiometric contamination, rain rates are derived. The land and coast algorithms use an empirical brightness temperature relationship to determine rain rates, and the ocean algorithm uses a Bayesian approach. The resulting swath data is passed through a uniformity check to filter noise and improve continuity between land and ocean retrievals.
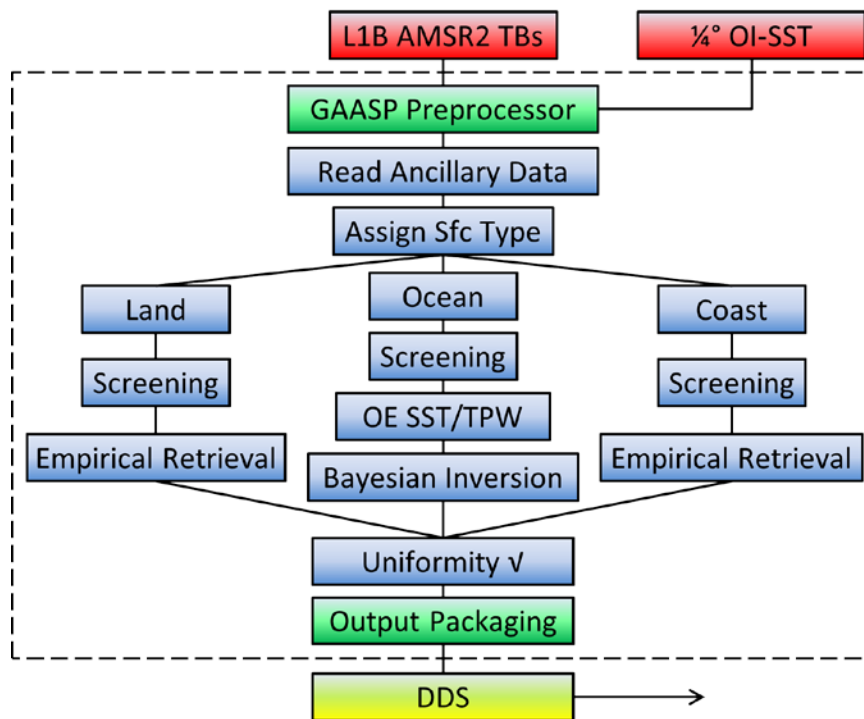

Figure 2-1: Processing outline for GPROF. The dashed box represents the GAASP system.

2.2. Algorithm Input

GPROF requires AMRS2 brightness temperatures between 10GHz to 89GHz at their native resolutions. The only dynamic ancillary data needed is a daily SST file. The most recent OI-SST analysis is supplied through DDS and sets boundary conditions for rain retrievals over oceans. The daily OI-SST near real-time analysis blends AVHRR SST observations and bias corrects relative to ship and buoy observations (Reynolds et al. 2007).

2.3. Theoretical Description

Radiometric characteristics of land and ocean greatly vary, which necessitates unique algorithms for rain rate retrievals over each of these surface types.

2.3.1. Physical Description

Ocean

The GPROF ocean rain rate is derived from a Bayesian retrieval scheme, comparing observed AMSR2 brightness temperatures to an a-priori database of TMI and TRMM Precipitation Radar (PR) measurements. GPROF's observationally generated database improves upon previous Bayesian algorithms that relied on cloud resolving models and contained representiveness errors. TMI and AMSR2 observe at similar frequencies, allowing for portability between satellite platforms.

The low surface emissivity allows for the detection of an emission signal from the raindrops themselves. The observed brightness temperature signature is compared to 2400 a-priori profiles with similar background SST and TPW. The SST is provided by the most recent Reynolds OI-SST analysis. TPW is calculated internally via a radiative transfer optimal estimation process described in Elsaesser and Kummerow (2008). The weighting of each a-priori profile is determined by the difference between observed and a-priori brightness temperatures.

Land

Rain rate retrievals over land are complicated by a dynamic and spatially variant surface emissivity, which precludes using a Bayesian inversion similar to the retrieval over oceans. Thus, an empirical approach dependent upon scattering of ice particles is necessary to calculate rain rates over land.

The first step in the land retrieval algorithm is classifying each pixel as raining / non-raining. Higher frequencies in the microwave spectrum, such as 89GHz on AMSR2, are more sensitive to scattering of surface emissions by suspended ice particles. The relative

magnitudes of the 24- and 89-GHz channels identify scattering and regions where precipitation is likely present (Grody 1991). Subsequent screening procedures are necessary to identify desert, semi-arid land, and snow surfaces using brightness temperature relationships and climatological conditions (Adler et al. 2003; Ferraro et al. 1998). Once a pixel has been determined to be raining, an empirically derived T89V – rain rate relationship is applied and combines the calculated contributions from stratiform and convective precipitation.

Coast

Retrievals over the coast are complicated by multiple surface types with vastly different emissivities within a single FOV. The coastal retrieval follows the land algorithm, other than additional screening procedures.

2.3.2. Mathematical Description

Ocean

The ocean algorithm is rooted in a Bayesian retrieval framework, where the probability of a rain profile R given a particular brightness temperature vector T_b is:

$$\Pr(R \mid T_b) = \Pr(R) \times \Pr(T_b \mid R)$$

where $\Pr(R)$ is the likelihood that the profile will occur and $\Pr(T_b \mid R)$ is the probability of T_b given a particular rain profile. $\Pr(R)$ is determined from a clustering analysis of a-priori profile database. $\Pr(T_b \mid R)$ is related to the difference between the observed and database brightness temperature vectors. The precipitation retrieval is essentially a weighted sum of rain rates from all a-priori profiles with a similar radiometric signature.

The a-priori database is separated into bins based on TPW (2 mm resolution) and SST (1°C). Approximately 2500 profiles are within each bin. Each a-priori profile R contains information on the brightness temperature vector T_{bS}, the likelihood of the profile in nature $\Pr(R)$, and the surface rain rate RR_R. The algorithm cycles through all profiles within the designated SST/TPW bin and calculates the profile's weight W_R as

$$W_R = P(R) \times \exp\left[-\sum_c E_c \left(T_{bSc} - T_{bOc}\right)^2 \right]$$

where c is the 10- to 89-GHz channels (both polarizations), E_c is the channel's pre-defined weight factor based on model and observation errors, and T_{bOc} is the observed brightness

temperature for the specified channel. The pixel's surface rain rate RR_{sfc} is determined by the weighted average over all profiles within the SST/TPW bin

$$RR_{sfc} = \frac{\sum_i W_{R_i} RR_{R_i}}{\sum_i W_{R_i}}.$$

Further details of the GPROF ocean algorithm and construction of the a-priori database can be found in Kummerow et al. (2001; 2011).

Land

The primary rain identification conditions are (1) T24V – T89V > 8 K and (2) T89H < 270 K. Prior to retrieving surface rainfall over land, each pixel is subjected to extensive screening to identify snow, desert, and semi-arid surfaces (Figure 2-2). Rainfall retrievals are not performed over deserts or where snow is climatologically expected based on historical IMS snow cover data. Heritage screening procedures (Grody 1991; Ferraro et al. 1998, Adler et al. 2003) are also used to separate raining and non-raining pixels (Figure 2-3).

The algorithm separately calculates convective and stratiform contributions, RR_{conv} and RR_{strat}, respectively, to the overall surface rain rate RR_{sfc}:

$$RR_{sfc} = RR_{conv}P(C) + RR_{strat}[1 - P(C)].$$

The convective probability *P(C)* is dependent on vertically polarized brightness temperatures at 10-, 37-, and 89-GHz, the local spatial variability of T89V, the presence of a local T89V minima, and the polarization difference at 89-GHz. The empirical functions for RR_{conv} and RR_{strat} were developed with collocated TMI and TRMM PR observations (Gopalan et al. 2010):

$$RR_{conv} = -0.00001177T_{89V}^3 + 0.008027T_{89V}^2 - 1.946T_{89V} + 182.68$$
$$RR_{strat} = -0.0708T_{89V} + 19.7$$

Given that this algorithm was developed for TMI, which has slightly different sensor characteristics than AMSR2, a linear ($AMSR2_{TMI} = m * AMSR2_{native} + b$) transformation was applied to the AMSR2 brightness temperatures (Table 2-1).
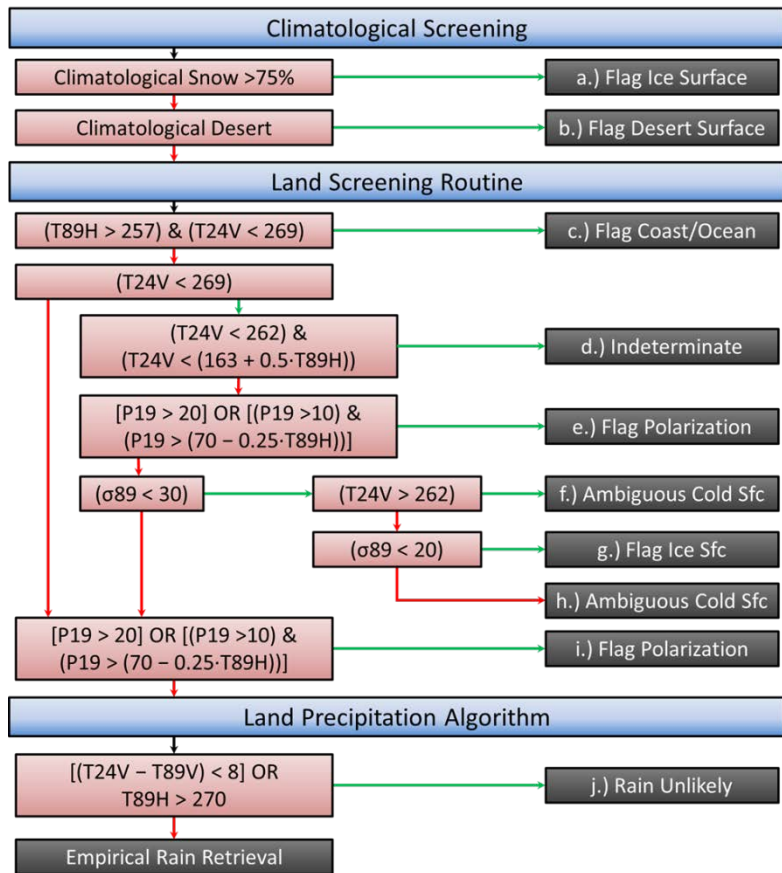
Figure 2-2: Screening procedure logic for GPROF. Green (red) arrows indicate that the conditions for flagging were met (not met).
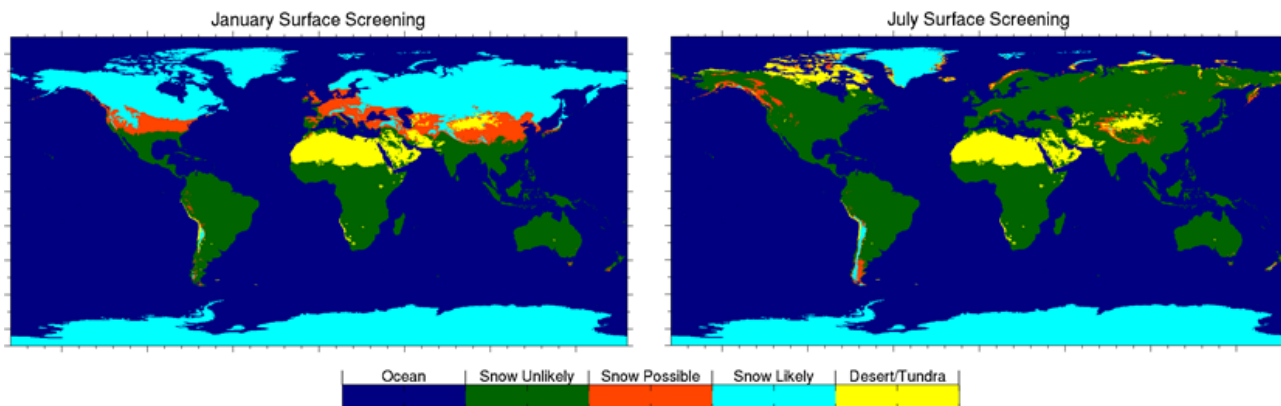

Figure 2-3: Screening regimes of GPROF2010V2 for January (Top) and July (Bottom). Regions where snow was climatologically likely were immediately flagged. Heritage screening procedures were used where snow was possible.

TMI *f*	AMSR2 *f*	*m*	*b*
10.7 V	10.7 V	0.9609	11.06
10.7 H	10.7 H	0.9509	14.18
19.4 V	18.7 V	0.9821	6.25
19.4 H	18.7H	0.9654	11.82
21.3 V	23.8 V	0.9989	0.06
37.0 V	36.5 V	0.9922	1.67
37.0 H	36.5 H	0.9705	8.74
85.5 V	89.0 V	0.9886	-0.11
85.5 H	89.0 H	0.9783	2.45

Table 2-1: Corresponding frequencies of TMI and AMSR2. Coefficients for translation from AMSR2 to TMI, with the form Tb(TMI) = m • Tb(AMSR2) + b.

2.4. Algorithm Output

EDR Output	Description	Dynamic Range	Size
Latitude	Observed latitude of 89A GHz FOV	-90.0 to 90.0°	486 × nscans
Longitude	Observed longitude of 89A GHz FOV	-180.0 to 180.0°	486 × nscans
Scan Time	Scan line start time [YYYY MM DD hh mm ss]		6 × nscans
surfaceType	10: Open Ocean 11: 100% Sea Ice 12: Partial Sea Ice 20: Land 30: Coast 31: Inland Water 32: Coastal Sea Ice		486 × nscans
surfaceRain	Surface rain rate (mm/hr)	0 to 100 mm/hr	486 × nscans
convectPrecipitation	Contribution of convective precipitation to total surface rain rate (mm.hr)		486 × nscans
qualityFlag	0: Good retrieval 1: Ambiguous retrieval 2: Low quality; No retrieval	[0, 1, 2]	486 × nscans

Table 2-2: Output structure of GCOM/AMSR2 Precipitation EDR

2.5. Performance Estimates

2.5.1. Test Data Description

GPROF for AMSR2 was primarily developed using AMSR-E's data record from 2002 to 2011. A year of AMSR2 observations prior to the official release of GCOM EDRs supplied an additional validation dataset.

2.5.2. Sensor Effects and Retrieval Errors

Nearly a year of observations has demonstrated that GCOM/AMSR2 is stable and producing consistent radiometric observations. There are no current concerns about geolocation errors or excessive sensor noise. Further detail about the calibration and validation can be found in the GCOM/AMSR2 SDR ATBD.

Variability of brightness temperatures due to sensor characteristics introduces 5% to 10% variation in rain rate measurements. Additional errors arise from inaccuracies in the radiative transfer model used to translate the TMI a-priori database to AMSR2 frequencies and FOVs. Advances in the forward model and characterization of surface emissivities will help reduce these errors.

Rainfall is an inherently difficult parameter to measure. Convection is a very localized process, such that the primary precipitating cloud only takes up a fraction of the overall FOV. Similarly, ground measurements (i.e. rain gauges) measure a single point while the satellite measures a 25 km^2 region. Thus, validation is complicated by the high temporal and spatial variability of rain. While point-by-point validation is possible, measurements of monthly accumulations reduce the noise associated with rain observations.

The TRMM Multi-satellite Precipitation Analysis (TMPA) synthesizes rain rate observations across several satellite platforms. These 3-hourly analyses effectively expand the latitudinal range of TRMM and provide near-global precipitation estimates. Direct comparisons between collocated TMPA (3B42), TMI (2A12), and AMSR2 (GPROF) rainfall rates verify that mission accuracy objectives are being met (Table 2-3).

Accuracy of rainfall retrievals over land is reduced by the complicated and variable nature of surface characteristics. Rough terrain, semi-arid land, and surface snow can produce a similar radiometric signal as rain. GPROF attempts to reduce error by omitting retrievals where desert or snow is climatologically likely. Heritage screening procedures are also used in an attempt to accurately flag the data. Future research in rain/no-rain classification will help to increase rainfall detection and reduce false alarms.

RMSE (mm·hr^{-1})	Land	Ocean	Overall
TMI & TMPA	3.1	1.2	1.6
AMSR2 & TMI	4.4	1.2	1.8
AMSR2 & TMPA	3.1	1.4	1.9

Table 2-3: RMSE of collocated instantaneous rain rate measurements from TMI, AMSR2, and TMPA over land and ocean regimes.

GPROF is not optimized for retrievals over the coast. The complex signature from multiple surface classes within a single FOV degrades quality of coastal retrievals. Any quantitative studies with AMSR2 rain retrievals over coastal regions should be done with caution.

2.6. Practical Considerations

2.6.1. Numerical Computation Considerations

The land algorithm is computationally efficient due to its simple regression calculation. The ocean algorithm is numerically simple, so rounding or truncation errors are not expected.

2.6.2. Programming and Procedural Considerations

The iterative optimal estimation (OE), which estimates TPW, cloud liquid water, and wind speed, is computationally and time intensive. The use of the external Reynolds SST product bypasses the need to internally calculate SST, which would add additional computation time. The time saved by pre-populating SST is applied to increase the profiles searched in the Bayesian search. All performance tests of the operational algorithm have met latency requirements.

2.6.3. Quality Assessment and Diagnostics

OSPO will maintain and monitoring and validation website with recent swath data. Comparisons between AMSR2 and TMI collocated measurements will be regularly made, in addition to side-by-side comparisons of global rainfall images. Monthly accumulations from GPROF will be compared to GPCC and GPCP monthly global analyses. Over CONUS, NMQ and Stage IV precipitation analysis will be used as daily validation sources.

2.6.4. Exception Handling

Fatal errors within GPROF result in no production of the precipitation EDR. Causes include read errors of ancillary files or SDR. Most ancillary files are static, so read errors are unlikely. Disruption of the Reynolds SST product for more than 14 days prohibits EDR production.

2.7. Validation

Global Precipitation Climatology Center (GPCC) Rain Gauges

The GPCC global network of rain gauges provides a ground-based system to validate GPROF retrievals (Schneider et al. 2011). Gauge estimates were compared to AMSR2 monthly rain retrievals from GPROF. Monthly estimates of rainfall from gauges were accumulated on a 2.5° x 2.5° grid for January to June 2013. Grid boxes with fewer than five

gauges were removed from the sample. Observations were highly concentrated over the United States, Western Europe, the East Asia, and coastal Australia, with sparse observations through much of South America, Africa, and Central Asia. GPROF accurately diagnosed global rain patterns (Figure 2-4), with root mean-square error (RMSE) of 1.7 mm·day^{-1} (Figure 2-5). There was not an observed annual cycle in GPROF accuracy when compared to the tropical and subtropical GPCC gauges.
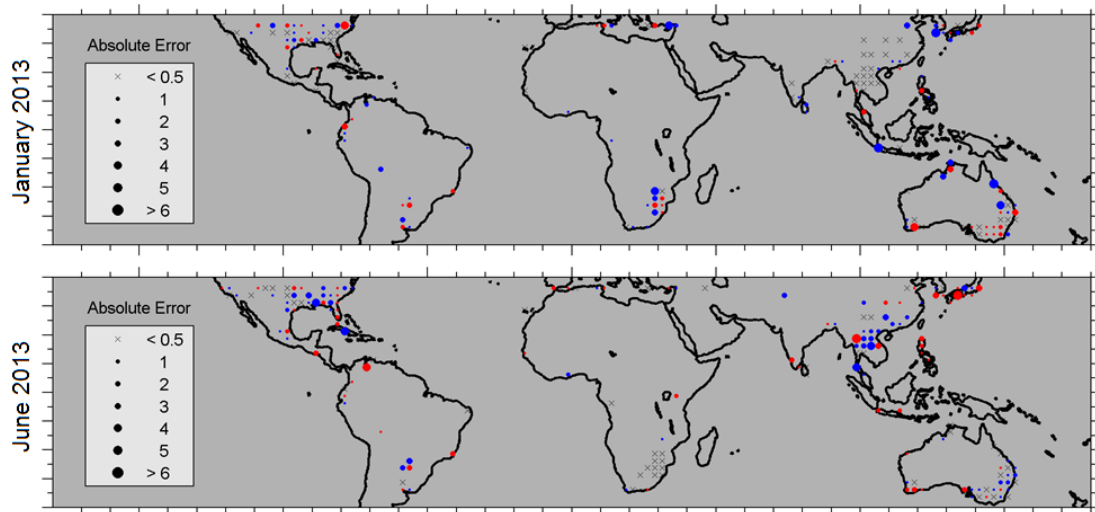

Figure 2-4: Overestimation (red) and underestimation (blue) of monthly accumulations of AMSR2 GPROF retrievals relative to monthly average GPCC measurements for January (top) and June (bottom) 2013.

Global Precipitation Climatology Project (GPCP) Monthly Analysis

The GPCP Version 2.2 Combined Precipitation Set merges monthly rain estimates from the GPCC gauge network and microwave and infrared satellites (Adler et al. 2003; Huffman et al. 2009). GPCP rain rate measurements reduce regime-based systematic errors in satellite retrievals, such as in snowy regions. GPCP analysis provide global climate data to validate GPROF retrievals on monthly timescales (Figure 2-6). GPROF performed well in convective regimes, including over South America and Africa. It accurately identified the spatial extent of precipitation and locations of local maxima and minima. A persistent problem with microwave retrievals is overestimation of rainfall over Africa and underestimation over South America. Screening updates in GPROF enhanced summer rainfall totals South America, bringing measurements closer to GPCP analysis. A similar increase to rainfall occurred over India during the summer monsoon season. Over the oceans, GPROF identifies the ITCZ and mid-latitude cyclone tracks. The comparisons shown here were derived from GPROF for AMSR-E.
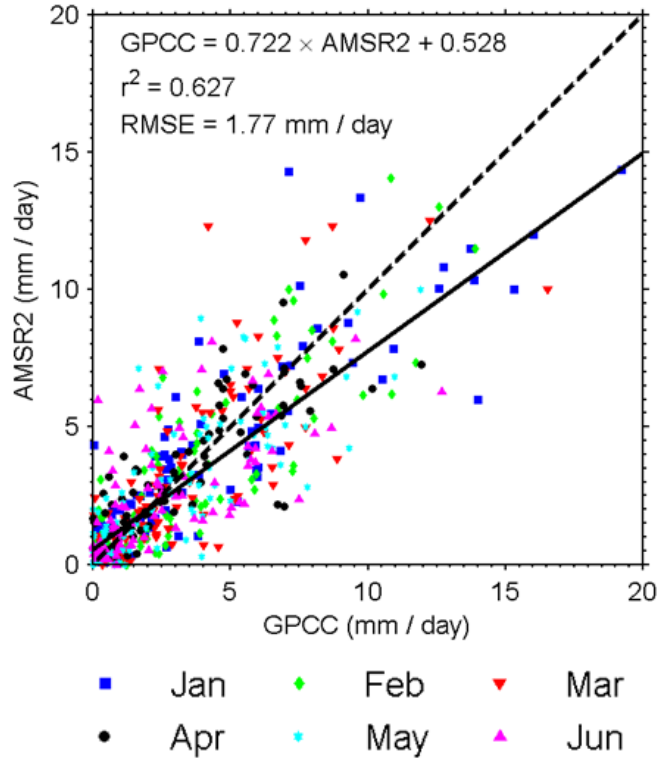
Figure 2-5: Comparison of GPCC and GPROF/AMSR2 monthly rain estimates for January to June 2013.
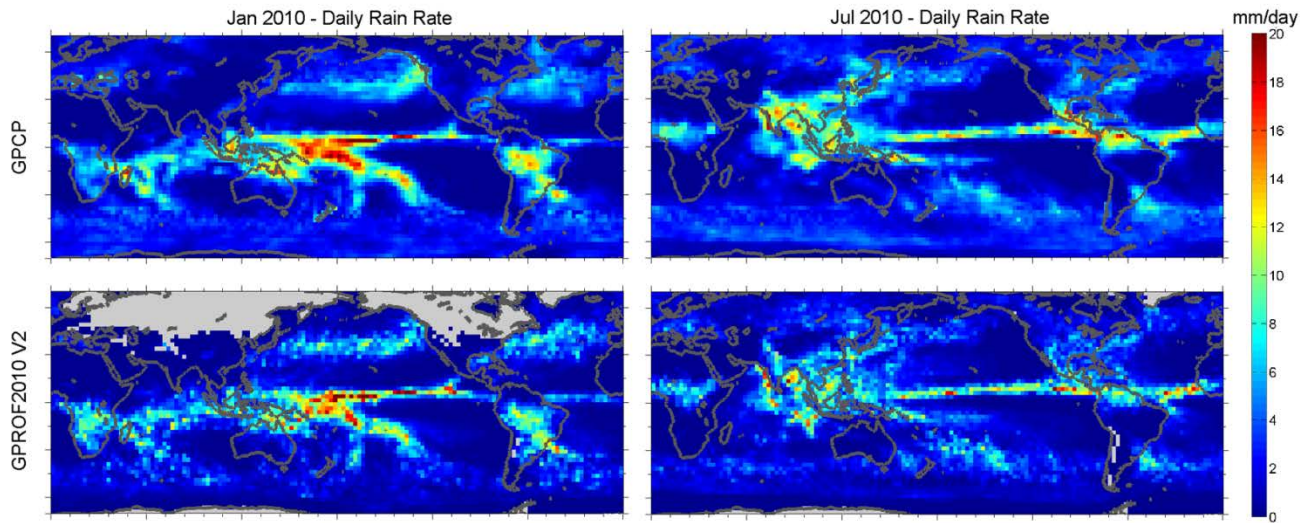

Figure 2-6: Comparison of GPCP monthly rain rate (top) and corresponding GPROF retrievals for AMSR-E in January (Left) and July (Right) 2010.

Tropical Rainfall Measurement Mission (TRMM) Comparisons

Given the lack of direct precipitation measurements over the open-ocean, satellite measurements drive the validation over ocean. The low-inclination orbit of TRMM allows for overlapping observations from the TMI and AMSR2 microwave imagers daily in the tropics. A previous version of GPROF is the operational algorithm for NASA's 2A12 Hydrometeor Profile product for TMI. Comparisons of collocated TMI and AMSR2 rain rate estimates (1 km, ± 30 minutes) show general agreement and similar histograms of rain rate distributions (Figure 2-7). Additionally, zonal means of TMPA, TMI, and AMSR2 show strong agreement between observational systems (Figure 2-8).
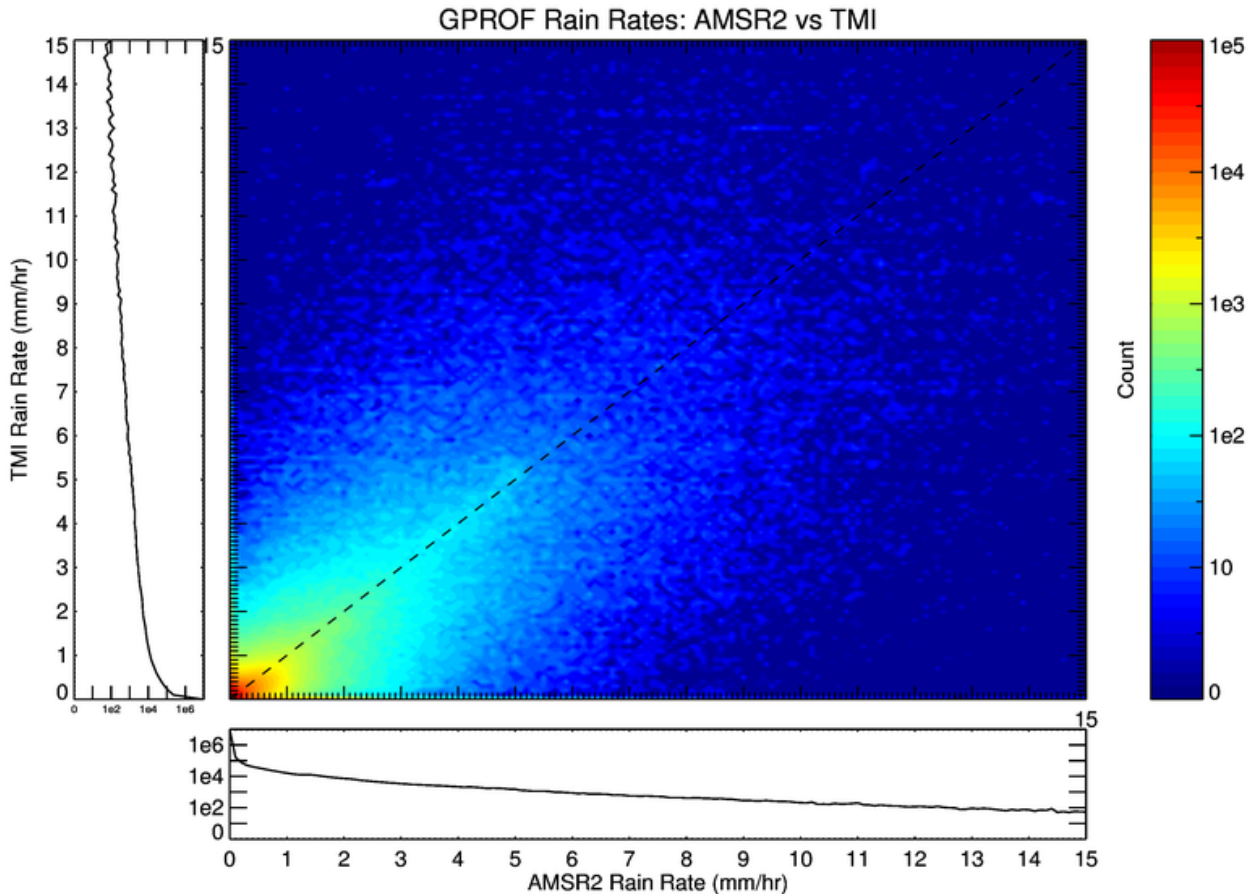

Figure 2-7: Density plot of collocated instantaneous rain rate estimates for TMI and AMSR2. Histograms along the axes show the rain rate distribution for each sensor.
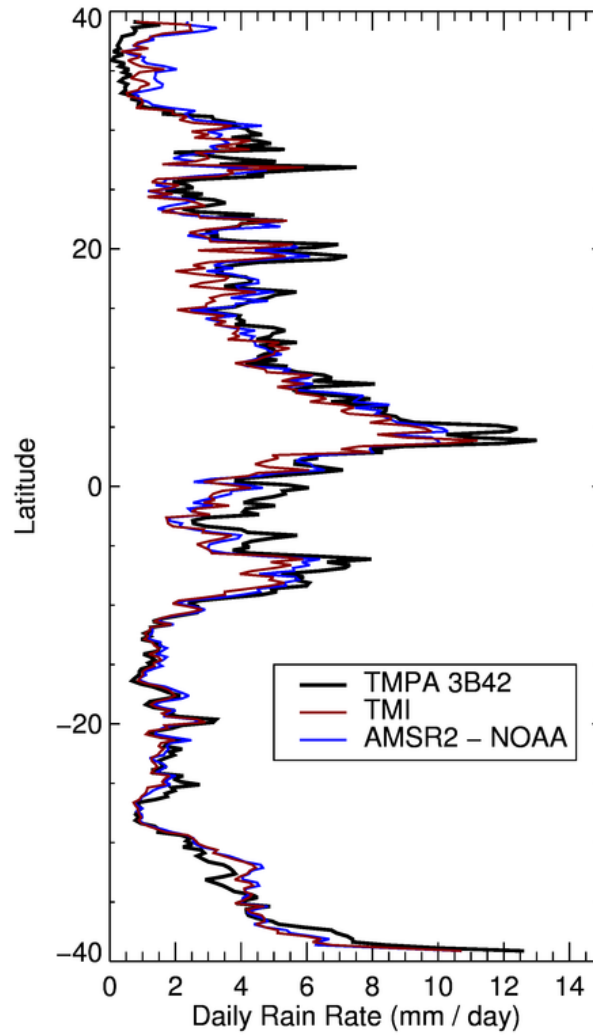
Figure 2-8: Zonal mean of collocated rain rates for TMPA (black), TMI (red), and AMSR2 (blue) for all surface classes.

3. ASSUMPTIONS AND LIMITATIONS

3.1. Performance Assumptions

The Bayesian rain rate retrieval over oceans assumes a representative sampling of PR profiles within the database. The low-inclination of TRMM limits observations in cold SST regimes. The lower atmosphere of observed tropical profiles is truncated to populate the database in poorly sampled regimes. The Modeling the translation of database brightness temperatures from TMI to AMSR2 frequencies and FOVS relies on an accurate radiative transfer model. Non-raining scenes are typically accurate to less than 1K (Kummerow et al. 2011).

GPROF assumes that the empirical relationship between brightness T85V and rain rate over land for TMI (Gopalan et al. 2010) is applicable to T89V for AMSR2. The linear correction applied to AMSR2 brightness temperatures should address this issue. The brightness temperature dependent screening procedures were developed from other passive microwave imagers and applied to AMSR2. Performance of the screening is assumed to be comparable between imagers.

3.2. Potential Improvements

The a-priori database for ocean retrievals will be improved with the launch of GPM in 2014. The higher inclination orbit compared to TRMM will create a more representative database containing observations over a wider SST and TPW range. Screening for surface snow contamination can be improved by using the operational daily IMS snow product to reduce the reliance on brightness temperature dependent screening procedures. Future iterations of GAASP will allow for data-sharing between EDR algorithms, ensuring consistent measurements across all AMSR2 products.

4. REFERENCES

Adler, R. F., G. J. Huffman, and P. R. Keehn. 1994. Global tropical rain estimates from microwave-adjusted geosynchronous IR data. *Remote Sens. Rev* **11**:125–152.

Adler, R.F., G.J. Huffman, A. Chang, R. Ferraro, P. Xie, J. Janowiak, B. Rudolf, U. Schneider, S. Curtis, D. Bolvin, A. Gruber, J. Susskind, and P. Arkin, 2003: The Version 2 Global Precipitation Climatology Project (GPCP) Monthly Precipitation Analysis (1979-Present). *J. Hydrometeor.*, **4**, 1147-1167.

Elsaesser, G. S., and C. D. Kummerow, 2008: Toward a fully parametric retrieval of the nonraining parameters over the global oceans. *J. Appl. Meteor. Climatol.*, **47**, 1599–1618.

Ferraro, R. R., E. A. Smith, W. Berg, and G. J. Huffman. 1998. A screening methodology for passive microwave precipitation retrieval algorithms. *J. Atmos. Sci* **55**:1583–1600.

GCOM-W1 "SHIZUKU" Data Users Handbook. First Edition. JAXA. January 2013. SGC-120011.

Gopalan, Kaushik, Nai-Yu Wang, Ralph Ferraro, Chuntao Liu, 2010: Status of the TRMM 2A12 Land Precipitation Algorithm. *J. Atmos. Oceanic Technol.*, **27**, 1343–1354.

Grody, N. C., 1991: Classification of snow cover and precipitation using the Special Sensor Microwave/Imager (SSM/I). *J. Geophys. Res.*, **96**, 7423–7435.

Huffman, G.J, R.F. Adler, D.T. Bolvin, G. Gu, 2009: Improving the Global Precipitation Record: GPCP Version 2.1. *Geophys. Res. Lett.*, **36**, L17808.

Imaoka, K., M. Kachi, M. Kasahara, N. Ito, K. Nakagawa, and T. Oki, 2010: Instrument Performance And Calibration Of Amsr-E And Amsr2. *Proc. Int. Archives of the Photogrammetry, Remote Sensing and Spatial Information Science*, **vol. XXXVIII**, Part 8.

Kummerow, Christian, and Coauthors, 2001: The Evolution of the Goddard Profiling Algorithm (GPROF) for Rainfall Estimation from Passive Microwave Sensors. *J. Appl. Meteor.*, **40**, 1801–1820.

Kummerow, Christian D., Sarah Ringerud, Jody Crook, David Randel, Wesley Berg, 2011: An Observationally Generated A Priori Database for Microwave Rainfall Retrievals. *J. Atmos. Oceanic Technol.*, **28**, 113–130.

Reynolds, R. W., T. M. Smith, C. Liu, D. B. Chelton, K. S. Casey, and M. G. Schlax, 2007: Daily high-resolution blended analyses for sea surface temperature. *J. Climate*, **20** , 5473-5496.

Schneider, Udo; Becker, Andreas; Finger, Peter; Meyer-Christoffer, Anja; Rudolf, Bruno; Ziese, Markus, 2011: GPCC Full Data Reanalysis Version 6.0 at 2.5°: Monthly Land-Surface Precipitation from Rain-Gauges built on GTS-based and Historic Data.

END OF DOCUMENT